NUMERICAL STUDY ON THE INFLUENCE OF AN ADIABATIC RECTANGULAR OBSTACLE IN A BACKWARD-FACING STEP FLOW

Décio L. Medeiros, decio.medeiros.22@gmail.com
Rogério G. Santos, roger7@fem.unicamp.br
University State of Campinas – UNICAMP, Mechanical Engineering Faculty, Zip Code: 13083-970, Campinas – SP, Brazil

Abstract. *Results for laminar two-dimensional backward facing step flow case with and without the presence of an adiabatic square cylinder obstacle is presented in this work. Location of the detachment point on the lower wall, as well as velocity profiles were obtained and compared between the cases. The goal is to identify the influence of the obstacle upon the flow behavior. A developed Fortran code that employs the UNIFAES method to discretize the advective and viscous fluxes of the Navier-Stoke equations is utilized in the simulations. The momentum equations are integrated after the solution of a Poisson pressure equation. The study utilizes a staggered uniform regular mesh. The results shows the effects of the obstacle presence upon the flow pattern.*

Keywords*: backward-facing step flow; rectangular obstacle; numerical simulation; UNIFAES*

1. INTRODUCTION

Flow separation occurs in channels with variable flow passage areas, resulting in detachment and reattachment of the fluid boundary layers in contact with the channel inner surface. The separation point is defined by the transition between forward and backward flow. The backward-facing step is a simple geometry often regarded as a benchmark study case for the phenomenon. The flow separation behavior influence the heat transfer efficiency in heating and cooling engineering applications, such as combustion chambers, heat exchangers and cooling of turbine blades. Furthermore, the flow detachment and bubble formation affects applications that involves mass transfer, for example a gas turbine.

In the literature, the backward-facing step problem was study extensively with both experimental and numerical approaches. A comprehensive review of experimental studies of laminar mixed convection flow over backward- facing is presented by Abu-Mulaweh (2003). Regarding numerical methods for two-dimensional backward-facing step flow solutions, general results shows the numerical methods tend to predict accurately enough the flow behavior until Reynolds numbers about 700. Erturk (2008) implements a stable and efficient numerical method based on the 2-d steady incompressible Navier-Stokes equations in stream function and vorticity formulation, presenting results for Reynolds number between 100 and 3000 based on the channel height.

Inserting a solid obstacle inside the backward-facing step flow channel enables the possibility to control important flow separation characteristics. Depending on the obstacle positioning, the recirculation zone length behind the step is affected by flow movement redirection. Selimefendigil and Oztop (2014) studied the influence of different vertical positions of a square in a laminar pulsating flow in order to control the flow behavior and the hear transfer.

The goal of this work is to compare results between the classic backward-facing case and specific determined cases that have the addition of a rectangular obstacle blocking the channel flow. The obstacle position will vary horizontally in order to control the recirculation zone length behind the step.

1. METHODOLOGY

The numerical simulation is realized utilizing our developed Fortran code. The algorithm based on the volume-finite method is responsible for discretizing and solving the incompressible non-dimensionalized Navier-Stokes equation. It employs the UNIFAES method (Unified Finite Approach Exponential-type Scheme) for the advective and diffusive terms spatial discretization. An explicit temporal discretization method is applied for the transient term. The momentum equations are integrated explicitly after the solution of a Poisson pressure equation that enforces mass conservation. The mesh is regular, uniform and staggered.

2.1 Mesh

The staggered regular uniform mesh (figure 1) has the pressure stored in the cell centers of the control volume, while the velocity components are located at the cell faces (Patankar, 1980). The study implement four meshes with different refinement degrees detailed on table 1.

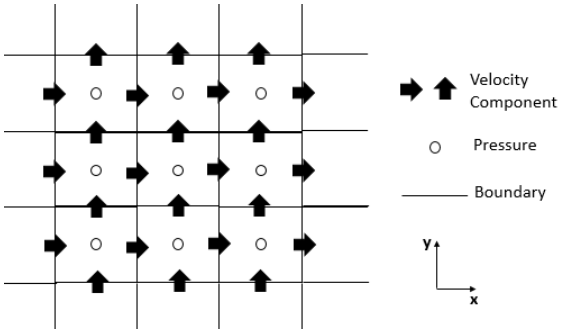

Figure 1. Staggered Mesh

Table 1. Meshes refinement

	Mesh 1	Mesh 2	Mesh 3	Mesh 4
Number of cells (x direction)	60	120	180	360
Number of cells (y direction)	40	80	120	120
Total number of cells	2400	9600	21600	43200

2.2 UNIFAES

The UNIFAES method (Unified Finite Approach Exponential-type Scheme) is employed for the discretization of the advective and diffusive terms. This scheme functions are obtained as exact solutions of a linear equation. Considering the two dimensional momentum equation in non-dimensional dummy variable ϕ:

$$\frac{\partial \phi}{\partial t} + Re\frac{\partial (u\phi)}{\partial x} + \frac{\partial (v\phi)}{\partial x} - \frac{\partial^2 \phi}{\partial^2 x^2} - \frac{\partial^2 \phi}{\partial^2 y^2} = S \tag{1}$$

The exponential-type schemes use as interpolation curve the exact solution of the one-dimensional equation:

$$Re\, u\frac{\partial (\phi)}{\partial x} - \frac{\partial^2 \phi}{\partial^2 x^2} = K \tag{2}$$

The class of exponential-type schemes started with Allen and Southwell (1955) finite differencing exponential scheme. The first exponential schemes proposed in the finite volume approach (Spalding, 1972) were based on a homogeneous generating equation (meaning that in Eq. 2 the variable K equals to zero). Schemes utilizing a non-homogeneous generating equation and the finite volume approach include the Locally Analytic Differencing Scheme, LOADS, (Wong and Raithby, 1979), Flux-Spline Scheme, (Varejão, 1979), and, the scheme discussed in more details here, the Unified Finite Approaches Exponential-type Scheme, UNIFAES (Figueiredo, 1997).

According to Leonard and Drummond (1975), all exponential-type schemes are asymptotically second order, but at high Reynolds number the schemes based on the homogenous generating equation approach the first order upwind scheme, whereas the exponential-type finite volume schemes based on nonhomogeneous generating equations are effectively second order at any Reynolds number. However, the greater computational time spending of the exponential function is a problem that motivated the development of approximations such as the Power-Law Scheme (Patankar, 1980) and Padé approximants (Axelsson and Gustafsson, 1979).

UNIFAES was initially submitted to a series of tests representing eigenfunctions of the linear advective-diffusive transport equation on a uniform flow field (Figueiredo, 1997). It showed stability even at Peclet numbers as high as 109 and very good accuracy in all eigenfunctions, generally overcoming the central differencing, the simple exponential and LOADS. The UNIFAES was later submitted to the Smith and Hutton test problem for Peclet numbers up to 106, concerning the transport of a scalar in a prescribed curved velocity field, presenting again good performance (Figueiredo and Llagostera, 1999).

The Finite Volume Exponential-type Scheme for discretizing the advective and viscous transport of momentum, using the UNIFAES method is formulated below. More detailed algebraic formulations can be found in (Figueiredo, 1997; Figueiredo and Llagostera, 1999).

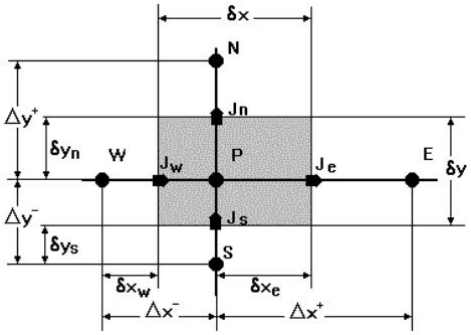

Figure 2. Discretized control volume.

The two dimensional control volume with the usual finite volume notation is represented in Fig.2. The variables $J_e, J_w, J_n \; and \; J_s$ represents the advective-viscous fluxes located at the cell faces. The variable P is the pressure stored in the cell center. The spatial variables illustrated above define the dimensions of the cell $(\partial x, \partial y)$, the distance between the cell center and each cell face $(\partial y_n, \partial y_s, \partial x_e, \partial x_w)$ and the distance between the center of this specific cell P and each of your neighbors W, E, N and S $(\Delta x^-, \Delta x^+, \Delta y^+, \Delta y^-)$.

The combined net advective and viscous flux are defined as A_ϕ.

$$A_\phi = Re\frac{\partial(u\phi)}{\partial x} + \frac{\partial(v\phi)}{\partial x} - \frac{\partial^2\phi}{\partial^2 x^2} - \frac{\partial^2\phi}{\partial^2 y^2} \tag{3}$$

For control volume locally analytic schemes the integrated net flux is given by:

$$\iint A_\phi \, dv \cong a_E(\phi_E - \phi_P) + a_W(\phi_W - \phi_P) + a_N(\phi_N - \phi_P) + a_S(\phi_S - \phi_P) - \psi \tag{4}$$

Where each element is defined as:

$$a_{E/W} = \pi\left(\pm p_{e/w}\right)\delta y/\delta x^{\pm} \tag{5}$$

$$a_{N/S} = \pi\left(\pm p_{n/s}\right)\delta x/\delta y^{\pm} \tag{6}$$

$$p_{e/w} = Re \; u_{e/w} \; \Delta x^{\pm} \tag{7}$$

$$p_{n/s} = Re \; v_{e/w} \; \Delta y^{\pm} \tag{8}$$

$$\pi(p) = \frac{p}{\exp(p) - 1} \tag{9}$$

$$\psi = [K_e\Delta x^+\chi(\mathrm{p_e}) - K_w\Delta x^-\chi(\mathrm{p}_w)]\delta y + [K_n\Delta y^+\chi(\mathrm{p}_n) - K_s\Delta y^-\chi(\mathrm{p}_s)]\delta x \tag{10}$$

$$\chi(\mathrm{p}) = \frac{\pi(p) - 1}{p} + R \tag{11}$$

$$R = \frac{\delta x_{e/w}}{\Delta x^{\pm}} \quad or \; R = \frac{\delta y_{n/s}}{\Delta y^{\pm}} \tag{12}$$

In the equations above, indexes e and n correspond to sign +, and indexes w and s correspond to sign -.

The modelling of K determine different schemes. In UNIFAES this information is obtained by differencing approach that led to the Allen and Southwell scheme (Allen and Southwell, 1955). Generalizing the Allen and Southwell exponential scheme K is defined as:

$$K_p = (\phi_P - \phi_E)\Pi^+ + (\phi_P - \phi_W)\Pi^- \tag{13}$$

The variable $\Pi^{\pm}$ for uniform grids according to Llagostera and Figueiredo (2000a,b):

$$\Pi^{\pm} = \frac{\pi(\pm p_u^{\pm})}{\Delta x^2} \tag{14}$$

where

$$p_u^{\pm} = Re\, u_p\, \Delta x \pm \tag{15}$$

2.3 Numerical Setup

The case of study (fig.3) is a channel with total length L, total height H and near of its entrance a backward-facing step with length c and height s. The rectangular obstacle (when present) has length ox, height oy and is positioned longitudinally symmetric to the x-axis and horizontally distant d from the step's end. The dimensionless values for these geometric properties where defined as: $L = 15, H = 1, c = 5, s = 0{,}5, ox = 0{,}5, oy = 0{,}25, d = 2\ or\ 4$.

The Reynolds number was defined by the characteristic dimension $(H - s)$, which corresponds to the value of the channel entrance height. The Reynolds numbers used in the simulations were $Re_1 = 400, Re_2 = 500, Re_3 = 600$. Three simulations cases (one without obstacle, one with obstacle and $d = 2$, one with obstacle and $d = 4$) were studied for each of these Reynolds numbers. Thus, in total we have these different setups simulated for each mesh refinement mentioned before.

Furthermore, results for velocity profiles and the length x_1 (fig.4) of the eddy behind the step that correspond to the recirculation zone were obtained for all the cases mentioned. The length of the recirculation zone on the lower wall (detachment point position) is normalized by the step height s (Lee and Mateescu, 1998).

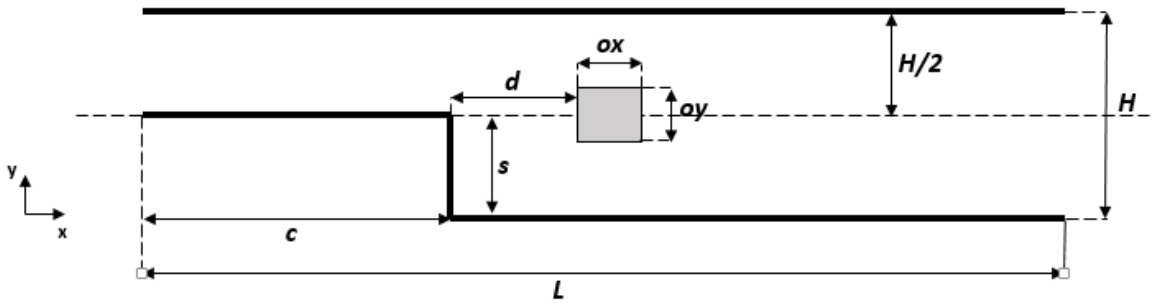

Figure 3. Geometry model

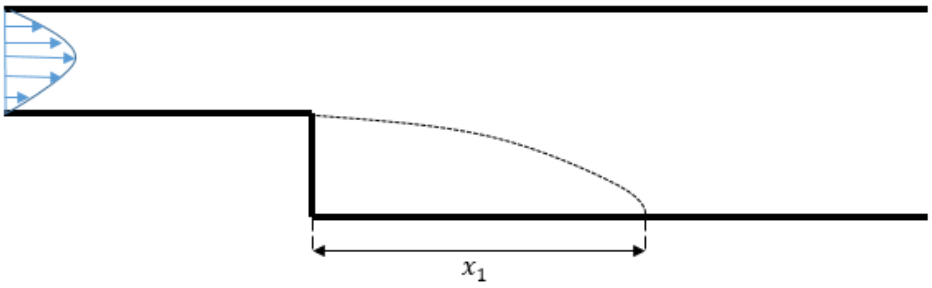

Figure 4. Recirculation zone length x_1

3. RESULTS

The results displayed in this section were obtained utilizing the most refined meshes (mesh 3 for $R_e = 400$ and $R_e = 500$; mesh 4 for $Re = 600$). The other meshes (1 and 2) data were calculated only as refinement test cases, considering that results should be less than 3% of difference if compared to the final values. Figure 5 shows the velocity component u field for $Re = 500$ in each of the three study cases: classic backward-facing step flow without obstacle and backward-facing step flow with a rectangular obstacle positioned inside the channel for the distances $d = 2$ and $d = 4$ between the step face and the obstacle frontal face.

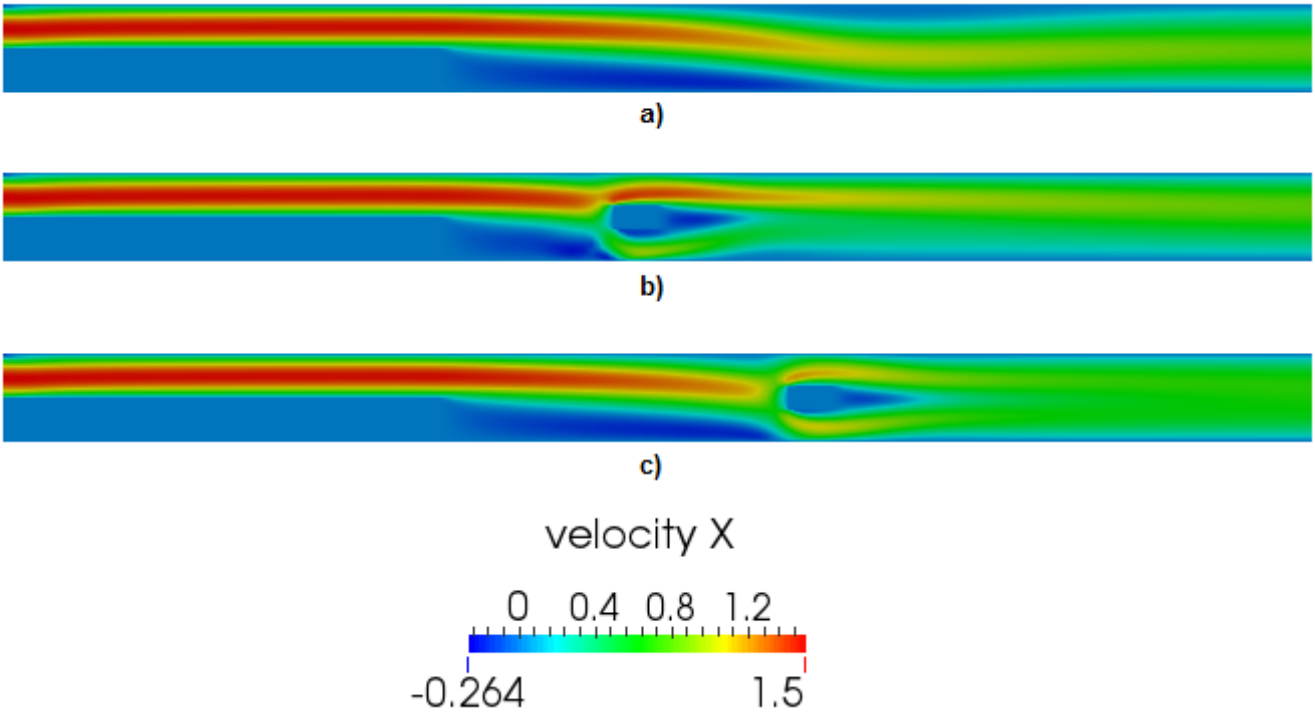

Figure 5. Velocity component x for Re =500. a) Classic backward-facing step flow. b) Backward-facing step with obstacle, d = 2. c) Backward-facing step with obstacle, d = 4.

Negative u velocities characterize the recirculation zone behind the step. The presence of the obstacle redirects the flow movement and reduces the length of the recirculation zone. The effects of the obstacle presence are more noticeable when the distance between the step and the obstacle equals 2 (Figure 5b). The recirculation area height drops abruptly when nearing the obstacle, whereas in the case without the obstacle the height decreases smoothly and almost in a linear pattern.

The behavior of the obstacle upon the recirculation region is further verified by the value $\left(\frac{x_1}{s}\right)$ obtained for each simulation case. Three different Reynolds numbers ($Re = 400, Re = 500\ and\ Re = 600$) were considered. The results shown in table 2 reaffirm the fact the obstacle presence reduces the recirculation zone length for both Reynolds numbers and distances from the step. The obstacle influence reduces as the distance from the step increases, until the point that the amount is barely considerable. Another important result obtained is the positive correlation between the Reynolds number and the recirculation length reduction.

Table 2. Normalized recirculation zone length (x_1/s) and length reduction results

Study Case	Reynolds Number (Re)	Obstacle Distance (d)	$\frac{x_1}{s}$	Lenght Reduction (%)
1	400	no obstacle	8.14	-
2	400	2	4.02	50.6
3	400	4	7.53	15.1
4	500	no obstacle	9.23	-
5	500	2	4.06	56.0
6	500	4	7.73	36.9
7	600	no obstacle	10.33	-
8	600	2	4.09	60.4

Figure 6 shows the variation of the normalized position of the detachment point at the lower wall x_1/s in function of the Reynolds number for the backward-facing step flow without the presence of an obstacle. The numerical simulation has good agreement with the experimental data obtained by Lee and Mateescu (1998).

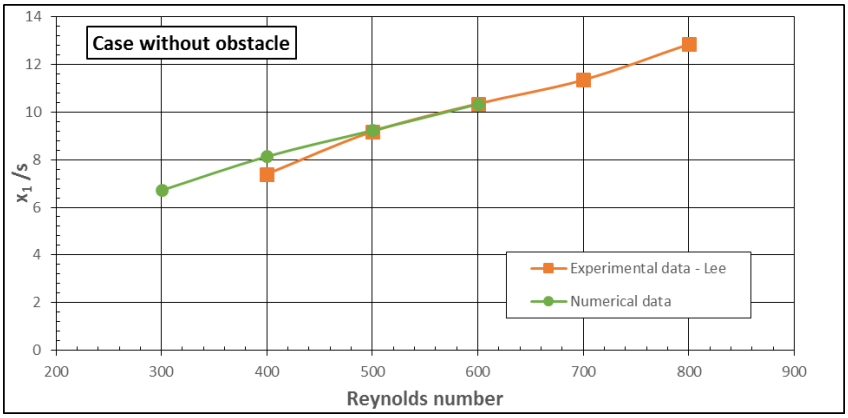

Figure 6. Variation of the normalized position of the detachment point at the lower wall x_1/s with Reynolds numbers. Comparison between numerical simulation and experimental data from Lee and Mateescu (1998).

The figures 7, 8, 9 and 10 show the profiles of the velocity u at different positions x for each of the cases with and without obstacle, the Reynolds number is 500.

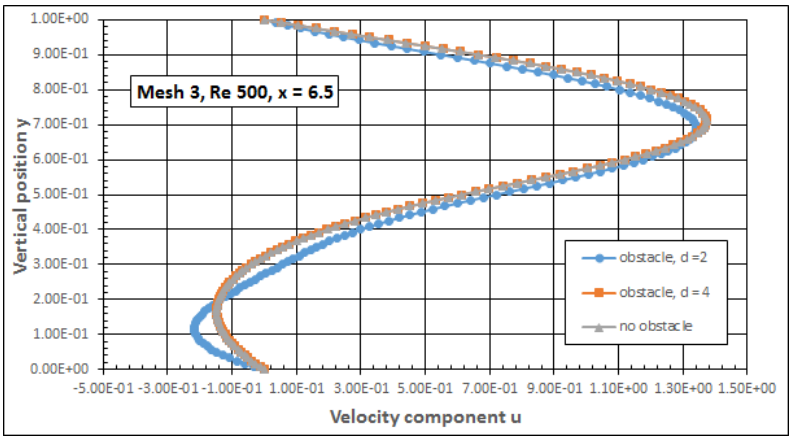

Figure 7. Re = 500, Velocity profiles of u component at x = 6.5 for cases with and without obstacle.

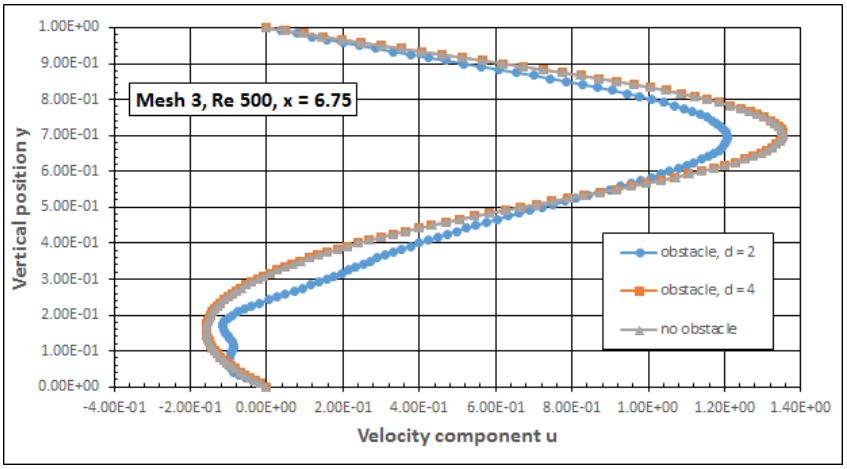

Figure 8. Re = 500, Velocity profiles of u component at x = 6.75 for cases with and without obstacle.

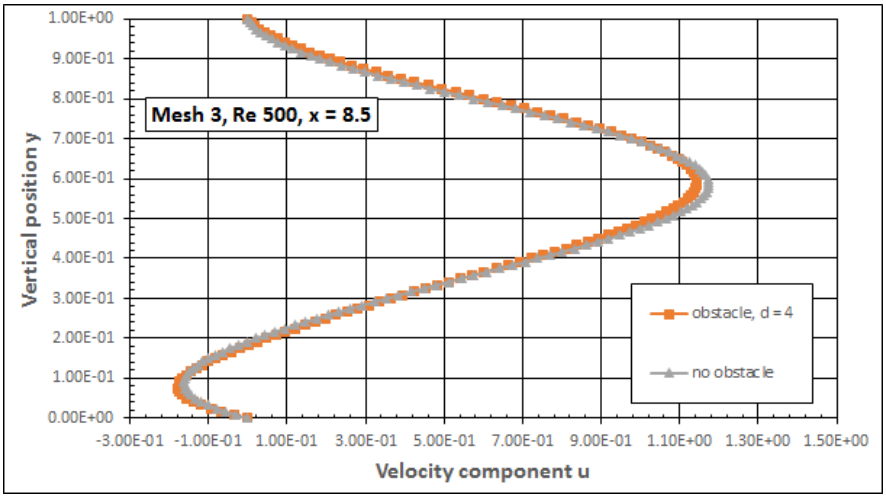

Figure 9. Re = 500, Velocity profiles of u component at x = 8.5 for cases with and without obstacle.

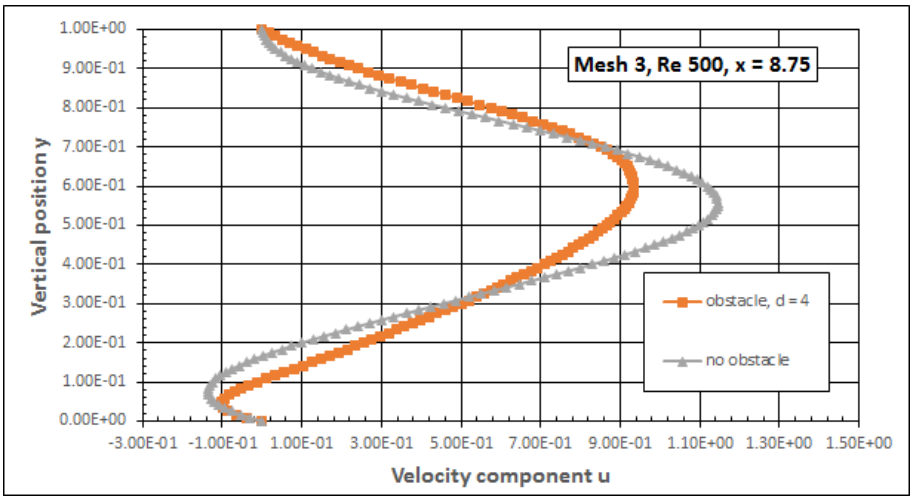

Figure 10. Re = 500, Velocity profiles of u component at x = 8.75 for cases with and without obstacle

When comparing figures 7($x = 6.5$) and 8($x = 6.75$) it is possible to identify that the obstacle impact in the results increases when the studied section x is closer to the obstacle position. The case for the obstacle with $d = 4$ from the step has almost no influence upon the velocity profiles located ate x = 6.5 and x =6.75. Figures 9($x = 8.5$) and 10($x = 8.75$) show the same behavior.

The velocity peak values are the first points to deviate between the cases. Considering as reference the non-obstacle backward-step facing case, it is noticed that the velocity profile variations at x = 6.5 (when d = 2) follow the same pattern as the velocity variations at x = 8.5 (when d = 4). The same can be implied if x = 6.75 (when d = 2) is compared to x = 8.75 (when d =4).

The result case displayed in figure 11 illustrates (for $Re = 600$) the difference between the flow behavior in a backward-step facing channel with the obstacle presence ($d = 2$) and in other without it. For the first case (Fig. 11a), two recirculation zones are identified, one in the channel lower wall (right beside the step) and another in the channel upper wall. However, in the case where the obstacle is present (Fig. 11b), the recirculation zone beside the step suffers a reduction in length size (table 2 has the comparison) and there is no recirculation zone visible in the channel upper wall. Instead, another recirculation zone was formed in the channel lower wall and there is some recirculation around the bottom of the obstacle.

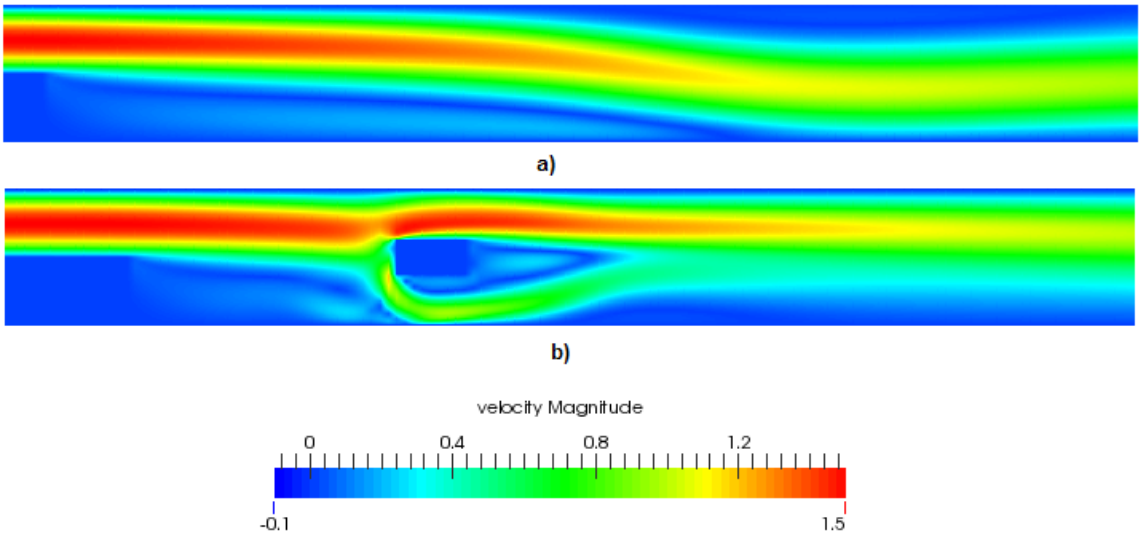

Figure 11. Velocity component x for Re =600 (zoomed in the region next to the step). a) Classic backward-facing step flow. b) Backward-facing step with obstacle, d = 2.

4. CONCLUSIONS

Numerical simulations were conducted in order to obtain the effects of positioning a rectangular obstacle inside a backward-facing step flow channel for three different Reynolds numbers. Two different obstacle horizontal positions were considered ($d = 2\ and\ d = 4$). The UNIFAES exponential scheme was employed as the standard discretization method for the Navier-Stokes equations.

First, the classical backward-facing step case was approached. The results for this case showed good agreement with experimental data present in the literature (Lee and Mateescu, 1998) regarding the flow separation behavior and recirculation zone formation. The accuracy of the numerical method implemented was satisfactory. The results were stable until Reynolds number of 600.

The recirculation zone length behind the step (lower wall detachment point) and the flow velocity profile change after positioning a rectangular obstacle inside the channel. When the obstacle is located closer to the step ($d = 2$) the recirculation zone length reduction is greater and the changes upon the velocity profile more significant. The obstacle presence had less impact when the distance from the step increased ($d = 4$). The Reynolds number showed to be a factor, as it was positively correlated with the reduction percentage in the recirculation zone length.

The presence of a rectangular obstacle inside a backward-facing step flow channel redirects the flow overall movement and can be used to control the recirculation zone length behind the step, and thus the flow separation main characteristics (detachment and reattachment points). More possibilities regarding the obstacle position, size and geometrical aspects can be checked in further work.

5. REFERENCES

Abu-Mulaweh, H., 2003. "A Review of Research on Laminar Mixed Convection Flow Over Backward- and Forward Facing Steps". *Int. J. Therm.* Sci., 42, pp. 897–909.

Allen, D.N.d.G. and Southwell, R., 1955. "Relaxation methods applied to determine the motion, in two dimensions, of a viscous flow past a fixed cylinder". *Quart. J. Mech. And Applied Math.*, Vol. 8, pp. 129-145.

Axelsson O. and Gustafsson I., 1979. "A modified upwind scheme for convective transport equations and the use of a conjugate gradient method for the solution of non-symmetric systems of equations". *J. Inst. Maths. Applics*, 23:321-337.

Erturk E., 2008. "Numerical solutions of 2-d steady incompressible flow over a backward-facing step, Part I: high Reynolds number solutions". *Comput Fluids*, 37, pp. 633-55.

Figueiredo, J.R., 1997. "A unified finite-volume finite-differencing exponential-type convective-diffusice fluid transport equations". *J. Braz. Society Mech. Sci.*, Vol.3, pp. 371-391..

Figueiredo, J.R. and Llagostera, J., 1999 "Comparative study of the unified finite approaches exponential-type scheme (UNIFAES) and its application to natural convection in porous cavity". *Numerical Heat Transfer, B,* Vol. 35, 347-367.

Lee, T. and Mateescu, D., 1998. "Experimental and numerical investigation of 2-D backward-facing step flow". *JOURNAL OF FLUIDS AND STRUCTURES,* Vol. 12, No. 6, pp. 703-716.

Leonard B. P. and Drummond J. E., 1975. "Why you should not use 'hybrid', 'power-law' or related exponential schemes for convective modelling – there are much better alternatives". *Int. J. Numerical Methods in Fluids*, 20:421-442.

Llagostera, J. and Figueiredo, J.R., 2000a. "Application of the UNIFAES discretization scheme to mixed convection in a porous layer with a cavity, using the darcy model". *J. Porous Media,* Vol. 3, No. 2, pp. 139-154.

Llagostera, J. and Figueiredo, J.R., 2000b. "Numerical study on mixed convection in a horizontal flow past a square porous cavity using UNIFAES scgeme". *J. Braz. Soc. Mech. Sci.,* Vol 4, pp. 583-597.

Patankar, S. V., 1980. "Numerical Heat Transfer and Fluid Flow, Numerical Heat Transfer and Fluid Flow*". McGraw-Hill*.

Selimefendigil F. and Oztop, H. F., 2014. "Control of Laminar Pulsating Flow and Heat Transfer in Backward-Facing Step by Using a Square Obstacle". *Journal of Heat Transfer*, Vol. 136.

Spalding D. B., 1972. "A novel finite difference formulation for differencial expressions involving both first and second derivatives". *Int. J. Numer. Meth. Eng*., 4:551-559.

Varejão L. M. C., 1979. "Flux-Spline Method for Heat and Momentum Transfer*". Ph.D. thesis*, University of Minnesota.

Wong H. H. and Raithby G. D., 1979. "Improved finite-difference methods based on a critical evaluation of the approximation errors". *Numerical Heat Transfer*, 2:139-163.

6. RESPONSIBILITY NOTICE

The author(s) is (are) the only responsible for the printed material included in this paper.